Life Sciences 280 (2021) 119671

Contents lists available at ScienceDirect

Life Sciences

journal homepage: www.elsevier.com/locate/lifescie

Role of autophagy and evaluation the effects of microRNAs 214, 132, 34c and prorenin receptor in a rat model of focal segmental glomerulosclerosis

Derya Yildirim [a,*], Onur Bender [b], Zehra Firat Karagoz [c], Fatma Helvacioglu [d], Mukadder Ayse Bilgic [e], Ali Akcay [f], Nuket Bavbek Ruzgaresen [g]

[a] Department of Internal Medicine, Ankara Education and Research Hospital, Ankara, Turkey
[b] Biotechnology Institute, Ankara University, Ankara, Turkey
[c] Department of Molecular Biology and Genetics, Bilkent University, Ankara, Turkey
[d] Department of Histology and Embryology, Faculty of Medicine, Baskent University, Ankara, Turkey
[e] Department of Nephrology, Medical Park Ankara Hospital, Ankara, Turkey
[f] Department of Nephrology, Koru Hospital, Ankara, Turkey
[g] Physician's Private Nephrology Clinic, Ankara, Turkey

ARTICLE INFO

Keywords:
Focal segmental glomerulosclerosis
Autophagy
miR-34c
miR-132
miR-214
Prorenin

ABSTRACT

Aims: Focal segmental glomerulosclerosis (FSGS) is the common cause of chronic renal disease worldwide. Although there are many etiologic factors which have common theme of podocyte injury conclusive etiology is not clearly understood. In this study, we aimed to explore the role of autophagy in the pathogenesis of podocyte injury, which is the key point in disease progression, and the roles of intrarenal microRNAs and the prorenin receptor (PRR) in the 5/6 nephrectomy and adriamycin nephropathy models of FSGS.

Main methods: For experimental FSGS model, 5/6 nephrectomy and adriamycin nephropathy models were created and characterized in adult Sprague Dawley rats. Microarray analysis was performed on FSGS and control groups that was confirmed by q-RT-PCR. Beclin1, LC3B, PRR, ATG7 and ATG5 expression were evaluated by western blotting and immunohistochemistry. Also, Beclin1 and PRR expression were measured by ELISA. Glomerular podocyte isolation was performed and autophagic activity was evaluated in podocytes before and after transfection with miRNA mimic and antagonists.

Key findings: Glomerular expression of Beclin1, LC3B, PRR, ATG7 and ATG5 were significantly lower in the 5/6 nephrectomy than adriamycin nephropathy group and in both groups lower when compared to control groups. Western blot results were consistent with immunohistochemical data. Electron microscopy revealed signs of impaired autophagy in FSGS. Autophagic activity decreased significantly after miR-214, miR-132 and miR-34c mimics and increased after transfection with antagonists.

Significance: These results showed that the role of autophagic activity and decreased expression of PRR in FSGS pathogenesis and miR-34c, miR-132 and miR-214 could be a potential treatment strategy by regulating autophagy.

1. Introduction

Focal segmental glomerulosclerosis is the more often glomerular reason of end stage renal disease which characterized by global sclerotic changes which may lead to irreversible loss of kidney functions. Currently, the diagnosis of FSGS is based on pathologic findings, clinical evidence and laboratory results. No available plasma and urine markers are available for diagnosing FSGS regarding delayed diagnosis.

Autophagy is a cellular homeostatic process that is responsible for degradation of damaged cellular proteins and organelles. This pathway involves formation of autophagic vesicles around of organelles and fusion of lysosomes that mediate enzymatic degradation [1]. Global deletion of autophagy pathway and impaired autophagic organelle turnover in podocytes cause manifestations of FSGS disease in animal models [2].

MicroRNAs (miRNAs) are a class of 22–24 nucleotide RNAs that

* Corresponding author at: Department of Internal Medicine, Ankara Education and Research Hospital, Hacettepe, Ulucanlar Cd. No:89, 06230 Altındag/Ankara, Turkey.
E-mail address: deryaakdeniz1@gmail.com (D. Yildirim).

https://doi.org/10.1016/j.lfs.2021.119671
Received 17 February 2021; Received in revised form 13 May 2021; Accepted 26 May 2021
Available online 1 June 2021

degrade mRNA and capable of translational repression. There is evidence that they can also lead to gene upregulation [3]. Strong evidences from research are emphasized that dysregulation of miRNAs may lead to some various diseases such as cancer, cardiovascular diseases, transplant rejection [4–7]. Also, some kidney diseases like Lupus nephritis, diabetic nephropathy, IgA nephropathy and polycystic kidney diseases were showed significant relation with miRNA functions [8–12].

Etiology of primary FSGS is not elucidated yet, a lot of studies showed significant relations with some miRNA molecules and FSGS disease [13–17]. Moreover, plasma miRNA markers were identified as novel biomarkers of FSGS [14]. Presence of miRNA molecules in pathogenesis of FSGS may provide new treatment options. miRNA mimics and antagonists may alter disease activity.

Prorenin receptor (PRR) is localized on the X chromosome, encodes a 37-kD transmembrane protein and is expressed in the central nervous system as well as in the heart, intestine and kidney, particularly in podocytes. It binds with prorenin to convert it into non-proteolytically activated prorenin that exerts renin enzymatic activity, thereby triggering the tissue renin angiotensin aldosterone system [15]. Previous reports exhibited that increased PRR and prorenin levels in the plasma or serum were associated with various diseases including cancer, hypertension, obesity, heart failure, diabetic nephropathy and glomerusclerosis [15–20]. Also stromal prorenin receptor is reported as essential for normal kidney development [21]. PRR is present on infiltrating lymphocytes and macrophages around glomeruli in anti-neutrophil cytoplasmic antibody (ANCA)-associated glomerulonephritis [22]. Previous studies have revealed that the serum levels of sPRR correlated with the degree of renal dysfunction in chronic kidney disease (CKD) patients [17] and also involved in mesangial fibrosis [23].

Considering all these, present data constitute the basis for the investigation of the functional role of miRNAs in the regulation of autophagy in the pathogenesis of FSGS caused by podocyte damage. This study aimed to investigate the role of autophagy in the pathogenesis of podocyte damage in vivo, which is a key point in disease progression in the FSGS, and intrarenal miRNA expression and PRR activity in autophagy regulation, to enable new treatment protocols.

2. Materials and methods

2.1. Experimental rat model

All experimental animal procedures were in accordance with the National Institutes of Health guide for the care and use of laboratory animals and local ethical committee approved the study. 48 male Sprague Dawley rats (6–8 weeks, 250–300 g) were used in the study. The rats were kept in cages in groups of 6 during the experiment in an environment with a humidity of 50–60%, a temperature of 22 ± 1 °C, 12 h night and 12 h daylight period. Animals divided into 4 groups; Sham, Adriamycin induced injury, 5/6 nephrectomy and control models. In 5/6 nephrectomy models secondary FSGS is performed. In the 5/6 Nephrectomy model (Secondary FSGS), rats (n = 20) were anesthetized and then entered into the abdominal area, the right kidney was separated from the surrounding tissue and carefully removed from the incision area. Renal blood vessels and ureter were cauterized, and the kidney was separated from the distal of the cauterization area. An infarct was created in approximately 2/3 of the left kidney by tying 2–3 branches of the left renal artery (Fig. 1).

In the control group (n = 6), sham operation was performed with laparotomy and mobilization of renal vessels. In the Adriamycin Nephropathy model (Primary FSGS) (n = 20), Adriamycin (Adriblastina, 10 mg vial) 4 mg/kg was injected intravenously (iv) from the tail twice every 14 days. The control group (n = 6) received iv saline injection. The purpose of using the two models here was to be able to monitor the changes in both Primary and Secondary FSGS and compare them with each other. Renal functions were monitored by measuring blood creatinine and albumin levels. Urine samples were also collected by using a metabolic cage and spot proteinuria were evaluated. The rats being nephrotic syndrome were sacrificed at the mean of 8th week in the 5/6 nephrectomy models (n = 14) and the 6th week in the Adriamycin nephropathy group (n = 14) in accordance with the literature [24–29].

2.2. Histological and immunohistochemical procedures

The kidneys were cut sagittal and put in a piece of formaldehyde for histopathological examination and a piece was divided into 1 mm3 pieces and stored in 2.5% glutaraldehyde (pH 7.4) with 0.1 phosphate buffer. Renal histology was examined by hematoxylene eosin staining. Immunohistochemical staining was performed on tissue samples to determine localization of selected autophagy markers in the kidney and compare the levels of controls and patient groups. For immunohistochemical staining, routine deparaffinization and rehydration procedures were performed on the 3 mm renal cortex sections. To inhibit endogenous peroxidase activity, 3% H_2O_2 (TA-125-HP, Thermo Scientific) solution prepared in PBS was applied to sections for 20 min. After the sections were kept in PBS for 10 min, the tissues were circled by hydrophobic pencil. Bovine serum albumin (TA-125-UP, Thermo Scientific) was placed on the slides and left for 20 min. Anti-PRR (ab40790), Abcam IncAnti-Beclin-1 (sc-11427, Santa Cruz Biotechnology), LC3B (3868, Cell Signaling) and ATG5 antibody (NBP1-76992, Novus Biologicals) which were prepared at 1/100 dilution and poured BSA onto the slide were incubated for 60 min with primary antibodies at 37 °C. After washing with PBS twice for 5 min, Biotinylated Goat

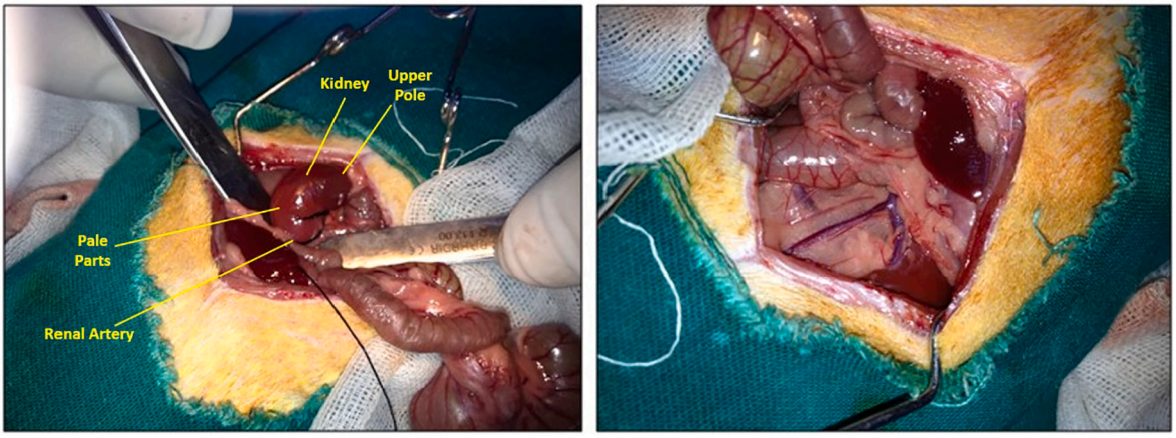

Fig. 1. Creating 5/6 Nephrectomy model. Left panel: The operation to create an infarct in approximately 2/3 of the left kidney by tying 2–3 branches of the left renal artery. Right panel: Pre-operative condition.

AntiPolyvalent was added to the sections for 15 min. After doing the same procedure with biotin containing secondary antibody, streptavidin peroxidase (TS-125-HR, Thermo Scientific) was placed and left for 15 min. Washed PBS again then DAB (TA-125-HD, Thermo Scientific) was dropped. Washing with PBS twice for 5 min and incubated in Mayers Hematoxylin (TA-125-MH, Thermo Scientific) for 3 min. Sections taken from PBS were allowed to turn blue. After washing in distilled water, it was shaken in 96% alcohol, was kept in 100% alcohol for 5 min and xylene for 5 min in 2 times. Histological scoring was performed by an experienced pathologist in immunohistochemical kidney tissue samples (OLYMPUS BX53). Accordingly, if the severity of staining is less than 25% for 1, 25–50% for 2, 50–75% for 3 and 75–100% for 4 points were scored.

2.3. Electron microscopic examination

Tissue samples which were fixed in 2.5% gluteraldehyde with 0.1 M phosphate buffer were washed 3 times with the buffer and left for 1 h with 1% osmium tetra oxide. Then the tissues that were activated to propylene oxide were embedded in the embedding material prepared with Araldit CY212 kit and blocks were prepared. At the end of the period, tissues passed through graded alcohol series. Semi-thin sections were taken from the polymerized blocks in a 560 °C for 48 h and stained with toluidine blue and examined under light microscope. Thin sections of approximately 0.5 μm from the marked regions were stained with uranyl acetate - lead citrate and evaluated on Carl Zeiss 906 E TEM.

2.4. Western blot analysis

Kidney tissues or podocytes were homogenized by using Tissue Ruptor in T-PER including protease inhibitor cocktail. Homogenized tissues were centrifuged at 20.000 rpm for 20 min at 4 °C. Supernatants were harvested and protein concentrations were measured by BCA protein assay kit (Thermo Scientific). Proteins were boiled in 4× laemmli sample buffer including 5% β-ME and subjected to 10% and 15% SDS-PAGE depending on the molecular weight of antibody, then transferred to PVDF membrane. Membranes were blocked with 5% skimmed milk powder in TBST for 1 h at RT and then hybridized with primary antibodies overnight at 4 °C, respectively: anti-Beclin-1 (3738, Cell Signaling), anti-LC3B (2775, Cell Signaling), anti-ATG5 (9980, Cell Signaling), anti-ATG7 (2631, Cell Signaling), anti-PRR (ab40790, Abcam Inc), anti-β-actin (Sc-47778, Santa Cruz Biotechnology). After washes with TBS-T, membranes were incubated with HRP conjugated secondary antibodies at RT for 1 h. Following incubation, membranes were washed with TBS-T and protein bands were visualized using ECL kit by Chemidoc MP (Bio-Rad).

2.5. Microarray analysis

Total RNA from FSGS model and control tissues were isolated with QIAzol Lysis Reagent (Qiagen) conventional guanidinium thiocyanate-phenol-chloroform method. miRNA expression profiling was performed in Affymetrix GeneChip miRNA 2.0 Arrays (901754, Affymetrix) system by using RNAs obtained from kidney tissues of FSGS model and untreated control rats according to the manufacturer's instructions. In brief, after the addition of poly-A tail to the RNA, 1 μg RNA per sample was labelled by using FlashTag Biotin RNA Labeling Kit (Genisphere). Hybridization, washing, and scanning of chips were performed according to the manufacturer's instructions.

2.6. Quantitative real-time RT-PCR

miRNA isolation was performed with miRNeasy Mini Kit (Qiagen) from tissues according to the manufacturer's instructions. miRNAs were reverse transcribed by using miScript II RT Kit (Qiagen) at 37 °C for 60 min and at 95 °C for 5 min according to the manufacturer's instructions. Quantitative real-time RT-PCR analysis was performed using miScript SYBR Green PCR Kit and miScript Primer Assay (Qiagen). The PCR mixture consisted of 2× QuantiTect SYBR Green PCR Master Mix (10 μl) which contains HotStarTaq DNA Polymerase, QuantiTect SYBR Green PCR Buffer, dNTP mix, including dUTP, SYBR Green I, ROX passive reference dye, 5 mM $MgCl_2$, 10× miScript Universal Primer (2 μl), 10× miScript Primer Assay (2 μl), RNase-free water (2 μl), and cDNA of samples (4 μl) in a total volume of 20 μl. PCR was performed with initial activation at 95 °C for 15 min, followed by amplification for 40 cycles, each cycle consisting of denaturation at 94 °C for 15 s, annealing at 55 °C for 15 s, extension at 70 °C for 30 s by using a Rotor-Gene Q real-time PCR cycler (Qiagen).

2.7. Primary podocyte isolation and culture

Primary podocyte cells were isolated from kidneys of 5/6 nephrectomy model rats. 5/6 nephrectomy model rats were fasted overnight and anesthetized with intraperitoneal injection of Ketamine hydrochloride: Xylazine (50 mg/kg:10 mg/kg). 4×10^6 dynabeads (4.5 μm) (Dynabeads M-450 Tosylactivated, Invitrogen) were prepared in 20 ml of ice-cold PBS and perfused to kidney vein very slowly. Ten minutes after perfusion, the kidney was extracted and placed in an ice-cold petri dish. Kidney was washed three times with ice-cold PBS, minced into small pieces and digested by shaking with 1 mg/ml collagenase (BD Biosciences) in PBS solution at 37 °C for 1 h. The specimens were then passed through a 100-μm cell strainer (BD Biosciences) two times and centrifuged at 900 rpm for 5 min at 4 °C. After removing the supernatant, 8 ml of ACK (Ammonium-Chloride-Potassium Lysing Buffer) was added to the pellet to eliminate the red blood cells. After thawing with ACK, the cells were centrifuged at 900 rpm for 5 min at 4 °C. The supernatant was discarded, and the pellet was dissolved in 2 ml of PBS. Tubes were placed on the magnet (Life technologies) for 15 min then discard the supernatant. The beads were washed 2 times with PBS by placing the tubes on a magnet for 15 min and discard the supernatant. The beads were resuspened in culture medium and seeded collagen coated dishes. Primary podocytes were cultured in DMEM/F-12 (1:1) (Hyclone, GE Healthcare) supplemented with 10% heat inactivated fetal bovine serum (Hyclone), 2 mM L-glutamine (Hyclone), 100 U/ml penicillin, 100 μg/ml streptomycin (Hyclone) and 2,5 μg/ml plasmocin (Invivogen) in a 5% CO_2 humidified incubator at 37 °C.

2.8. Transfection of miRNA mimic and antagonists to primary podocytes

After the microarray analysis and Q-RT-PCR validation, 30 nM selected miRNA (miR-34c, miR-132 and miR-214) mimics or antagonists (Qiagen) were transfected into primary podocytes (isolated from kidneys of 5/6 nephrectomy model rats) using Lipofectamine 2000 (Invitrogen) in OPTI-MEM I medium according to the manufacturer's instructions.

2.9. Statistical analysis

Data in the graphs are expressed as mean ± standard deviation in the form of mean bars and error bars. Non-parametric test was used for statistical analysis due to the low number of subjects in the groups. The relationship between the variables was evaluated by Mann-Whitney *U* test. Statistical significance level was accepted as $p < 0.05$. Statistical analysis of all data was performed using SPSS 20.0.

3. Results

3.1. Biochemical findings

When the biochemical values of 5/6 Nephrectomy, Adriamycin Nephropathy and Control rats were compared, it was found that serum creatinine levels of 5/6 Nephrectomy and Adriamycin Nephropathy

groups increased significantly compared to control rats (1.51 ± 0.01 mg/dl, 1. 46 ± 0.02 mg/dl and 0.43 ± 0.08 mg/dl, $p < 0.01$). Expressed as fold change, serum creatinine values increased 3.39 times in the Adriamycin Nephropathy group compared to the control, while it increased 3.51 times in the 5/6 Nephrectomy group. Serum albumin levels were significantly decreased in 5/6 Nephrectomy and Adriamycin Nephropathy groups compared to the control group (1.82 ± 0.47 g/dl, 1.94 ± 0.77 g/dl and 3.48 ± 0.33 g/dl, respectively, $p < 0.01$). The fold changes in serum albumin values; while the Adriamycin Nephropathy group decreased 1.79 times compared to the control, it decreased 1.91 times in the 5/6 Nephrectomy group. When urinary albumin/creatinine excretion rates of 5/6 Nephrectomy, Adriamycin Nephropathy and Control rats were compared; Urinary albumin/creatinine excretion rates of rats with FSGS model were found to be much higher than control mice (40.46 ± 8.37 mcg/mg, 38.74 ± 6.44 mcg/mg and 0.3 ± 0.14 mcg/mg, $p < 0.001$). The fold change values of the urinary albumin/creatinine excretion rates increased 129.1 times in the Adriamycin Nephropathy group and 134.8 times in the 5/6 Nephrectomy group compared to the control. There was no significant difference between serum creatinine, albumin levels and urine albumin/creatinine excretion rates between nephrectomy and adriamycin nephropathy groups ($p > 0.05$). These results are given in Table 1. Thus, it was observed that rats developed FSGS can be detected biochemically in the 8th week after 5/6 nephrectomy and in the 6th week in the adriamycin nephropathy model.

3.2. Histological and immunohistochemical observations

We used hematoxylene eosin staining method, which may help showing decreased number of nucleus and interstitial inflammation [30]. When hematoxylene eosin stained kidney sections were examined; control group showed normal renal histology (Fig. 2a). However, on the kidneys with FSGS, global and segmental sclerosis in the glomeruli, degeneration of tubules, cytoplasmic vacuolization, loss of brushy margins, proteinous material in some lumens, and atrophy in certain interstitium, interstitium edema cell infiltration and fibrosis were observed (Fig. 2b–c) which validated that the FSGS rat model has successfully created.

In the immunohistochemical staining with anti-Beclin-1, anti-LC3B, PRR and anti-ATG5 were observed in significantly reduced expression in both groups compared to controls in the surgical group (Fig. 3). Histological scoring was performed by an experienced pathologist, unaware of the experimental results, by taking the average number of stained cells in 10 different 400× microscope areas that did not overlap with each other. Protein expression was measured only from glomerular lesions. As seen in the Fig. 3m; results for anti PRR were 19.5 ± 3.6 in the controls, 9.4 ± 1.1 in the adriamycin nephropathy group and 4.2 ± 3.2 in the 5/6 nephrectomy group; anti-Beclin-1; the score in the control group was 25.6 ± 2.8, 11.4 ± 2.1 in the adriamycin nephropathy and 5.2 ± 2.3 in the 5/6 nephrectomy group; for anti-LC3B; while the score in the control group was 16.5 ± 4.6, for the adriamycin nephropathy group was 6.4 ± 1.13 and for the 5/6 nephrectomy group was 2.2 ± 1.2 and for anti-ATG5; 23.5 ± 4.8 in the control group, 13.6 ± 2.8 in the adriamycin nephropathy group and 3.2 ± 1.4 in the 5/6 nephrectomy group. Autophagy markers and PRR antibodies were significantly lower in adriamycin nephropathy and 5/6 nephrectomy group compared to control ($p < 0.01$). The difference between adriamycin nephropathy and 5/6 nephrectomy group scores were also significant ($p < 0.05$). According to the results of immunohistochemistry studies, decreased expression of PRR and autophagy markers Beclin-1, LC3B and ATG5 in the primary and secondary FSGS models suggests that autophagy may be associated with PRR expression and FSGS pathogenesis.

Table 1
Biochemical findings from Control, Adriamycin Nephropathy and 5/6 Nephrectomy Groups.

Parameters	Control (n = 6)	Adriamycin Nephropathy (n = 14)	5/6 Nephrectomy (n = 14)
Serum creatinine (mg/dl)	0.43 ± 0.08	1. 46 ± 0.02*	1.51 ± 0.01*
Serum albumin (gr/dl)	3.48 ± 0.33	1.94 ± 0.77*	1.82 ± 0.47*
Urinary albumin/creatinine excretion rates	0.3 ± 0.14	38.74 ± 6.44**, #	40.46 ± 8.37**, #

* Significantly different from control group ($p < 0.01$).

** Significantly different from control group ($p < 0.001$).

\# No significant difference between Adriamycin Nephropathy and 5/6 Nephrectomy groups ($p > 0.05$).

3.3. Electron microscopy observations

The glomerular structure of the renal cortex was evaluated at the electron microscope level for the control group and 5/6 nephrectomy. Especially glomerular basement membrane structure, podocyte cells, pedicle arrangement and autophagic vacuole formation were taken into consideration. In the control group, glomeruli showed normal structure in the semi-thin section passing through the kidney cortex (Fig. 4) while 5/6 nephrectomy samples showed a sclerotic appearance (Fig. 4d). Degeneration of podocyte cells was prominent compared to the control group. In some areas, excessive thinning of podocyte extensions was observed. In large and small growth, membrane-bound cellular residues and degenerate heterogeneous cell components that were not yet surrounded by membrane were distinguished in the primary extensions of podocytes. Electron-dense oval bodies were observed around the vacuole. These structures were accepted as indicators of autophagic activity. In some areas, the increase of mesengial cells observed in the advanced stages of FSGS. (Fig. 4e, f). Pedices on the basement membrane were completely erased in some areas (Fig. 4g) and the presence of degenerative mitochondria and autophagic vacuoles in the podocyte primary extension was detected in higher magnification of the square area (Fig. 4h). Another finding observed in this group was the formation of apoptotic bodies in podocytes with advanced cellular degeneration (Fig. 4i). Giant vacuoles were detected in the cytoplasm of some podocytes. It was observed that mitochondria were relatively increased in cells with this type of structural damage compared to the control group and had significant structural damage. Autophagic vacuoles were differentiated between degenerative mitochondrion (Fig. 4i). As a result, in the 5/6 nephrectomy group, structural damages compatible with focal segmental glomerulosclerosis were seen in the semi-thin and thin sections of the kidney. Irregular basal membrane thickness, fusion of pediceles, complete erosion in places, as well as increased mesengial cells with consisting advanced FSGS findings were observed. In addition to structural damage such as vacuole formation in podocyte cells, the presence of numerous degenerative mitochondria was determined. Significant structural damage was detected in glomerular endothelial cells and some podocytes in contrast to the control group. Formations of different stages of autophagy were observed as a sign of decreased autophagy in most areas of podocytes.

3.4. Protein expression levels of autophagic markers in experimental groups

Autophagy markers (Beclin-1, LC3B, ATG5, ATG7) and PRR were analyzed in both by surgically and adriamycin induced FSGS rats analyzed by western blotting (Fig. 5a). Acquired data were normalized against β-actin and analyzed by using ImageLab software (ChemiDoc MP, Bio-RAD). Results showed that there is a statistically significant decrease in protein level of autophagy markers in both surgically and Adriamycin induced FSGS groups compared to control group (Fig. 5b). p

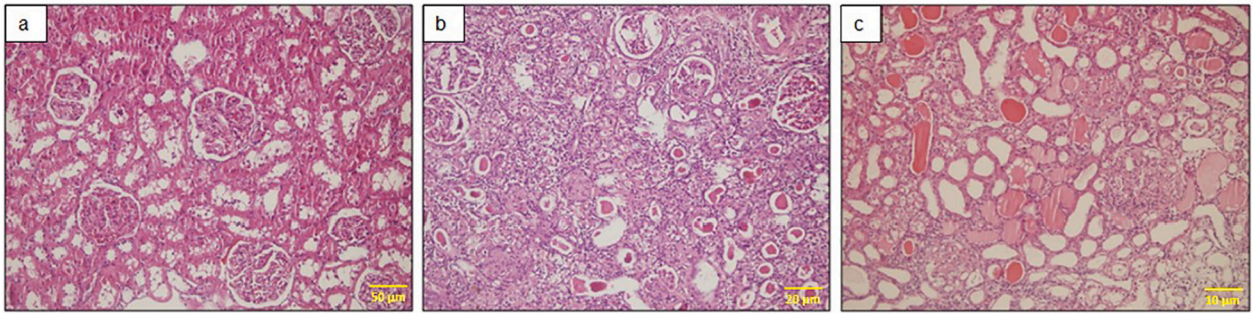

Fig. 2. Histopathological evaluation of experimental groups. a. Control group, hematoxylin eosin staining, ×40 magnification. b. 5/6 Nephrectomy group hematoxylin eosin staining, ×100 magnification. Global and segmental scleroses in glomeruli, degeneration in tubules, proteinaceous material and atrophy in some lumens, edema in the interstitium, significant mononuclear inflammatory cell infiltration and fibrosis. c. Adriamycin Nephropathy group hematoxylin eosin staining, ×200 magnification. Segmental scleroses in the glomeruli, glomeruli leading to one global sclerosis, degeneration in the tubules, cytoplasmic vacuolization, loss of brushy margins, some dilatation and proteinaceous material in the lumen, edema in the interstitium and a small number of mononuclear inflammatory cell infiltration.

value for surgically induced FSGS group is less than 0.01 while for Adriamycin induced FSGS group is less than 0.05. Also, all autophagy markers levels were observed in decreased expression in the surgical group compared to the adriamycin group ($p < 0.05$). Anti-PRR was used as the primary antibody for western blot analysis of PRR in renal tissue. PRR levels were decreased in the surgery and adriamycin groups compared to the controls ($p < 0.001$; Fig. 5c). The difference between surgery and adriamycin group was not statistically significant ($p > 0.05$).

3.5. Altered miRNA expression in the FSGS model

Microarray analysis revealed that differentially expressed miRNAs determined by in tissue samples of FSGS and control groups. In the 5/6 nephrectomy group, there was a significant increase in 19 miRNA expression and a significant decrease in 8 miRNA expression compared to the control (Fig. 6a). In adriamycin group, there was a significant increase in 15 miRNA expression and a significant decrease in 8 miRNA expression compared to control (Fig. 6b). A literature review for these miRNAs has been conducted and focusing on a total of 12 miRNAs that may play a role in the pathogenesis and autophagy regulation of FSGS. These miRNAs are miR-212, miR-132, miR-21, miR-146b, miR-130b, miR-34a, miR-34c, miR-18a, miR-376b-3p, miR-214, miR-192, miR-29c. Quantitative real-time PCR validation was performed for these miRNAs. Increased expression of miR-132 was about 7 and 11-fold, miR-34c was about 3 and 11-fold, and miR-214 was about 8 and 13-fold, respectively (Table 2). Considering the increasing potent expressions of these 3 miRNAs, we studied their mimic and antagonists.

3.6. Evaluation of the effect of selected miRNAs on autophagic activity

Autophagic activity was evaluated transfection with miR-34c, miR-132 and miR-214 mimics antagonists in podocytes. For this purpose, western blot studies were performed with anti-Beclin 1 (3738, Cell Signaling, USA), anti-LC3B (2775, Cell Signaling, USA), anti-ATG5 (9980, Cell Signaling, USA), anti-ATG7 (2631, Cell Signaling, USA) and anti-β-actin (Sc-47778, Santa Cruz Biotechnology, USA) antibodies (Fig. 7). After mimic transfections into primary podocyte cells, a statistically significant ($p < 0.05$) decrease was observed in all three miRNAs except Beclin-1 ($p > 0.05$) for miR-34c, LC3B ($p > 0.05$) for miR-132 and ATG5 for miR-214 ($p > 0.05$) compared to the control (Fig. 7). After transfection of miR34c, miR132 and miR214 antagonists, the expression of Beclin-1, LC3B, ATG5 and ATG7 increased significantly ($p < 0.05$), except for the increase in ATG7 following miR132 antagonist transfection compared to the control ($p > 0.05$) (Fig. 7).

3.7. Evaluation of the effect of selected miRNAs on PRR activity

Mimic and antagonist transfections of the 3 selected miRNA targets were performed as in the autophagic activity section, and then PRR protein levels were analyzed by western blot (Fig. 8). The expression levels of PRR were observed in significantly decreased after miR-34c, miR-132 and miR-214 mimic transfection compared to before transfection ($p < 0.01$). PRR expression increased significantly after transfection of miR-34c, miR-132 and miR-214 antagonists ($p < 0.05$).

4. Discussion

FSGS is the most common cause of nephrotic syndrome and significant cause of end stage renal disease. Classically, glomerulosclerosis refers to the matrix obliteration of the capillary lumen. FSGS can identify both a primary podocyte injury and a lesion that may develop due to non-immunologically adaptive secondary causes. In our study, we performed both the primary podocyte injury model, adriamycin nephropathy, and the secondary FSGS model with a significant decrease in the number of nephrons through 5/6 Nephrectomy. Both models are characterized by marked proteinuria and progressive renal failure and podocyte damage which is the common pathophysiological mechanism [31].

Autophagy is an essential pathway for cellular mechanisms. This process benefits by destroying misfolded proteins and nonfunctional organelles. Glomerular podocytes were identified as cells with high levels of basal autophagy [32]. Functional block of the autophagy machinery in podocytes by deletion of ATG5 caused a slowly progressing cellular degeneration [33]. Strikingly, some of the systemic manifestations of FSGS observed in humans are found in mice with mutations of autophagy pathway. The inhibition of autophagy pathway constitutes FSGS in mice [34]. In both primary and secondary FSGS models applied in our study; autophagic activity in podocytes have been shown to play an important role in the pathogenesis of FSGS. The decrease in autophagic activity was more observed in secondary FSGS. Then, in order to evaluate the specific effect of miRNAs on autophagic activity; our functional experiments have been shown to be a potential therapeutic strategy by controlling the expression of Beclin-1, LC3B, ATG5 and ATG7 proteins. Inhibition of these miRNAs with antagonists increased the expression of Beclin-1, LC3B, ATG5 and ATG7.

MicroRNAs, small noncoding RNA particles, opened a new road as unique biomarkers for tissue injury because of their tissue specifity and relative stability. Also, a lot of evidences proved that miRNAs in body fluid are reliable indicators of tissue damage [35–37]. miRNAs have been reported to play a role in kidney development and physiology, tubulointerstitial sclerosis development and progression [9,38–41]. Previous reports demonstrated some clinically significant miRNAs in

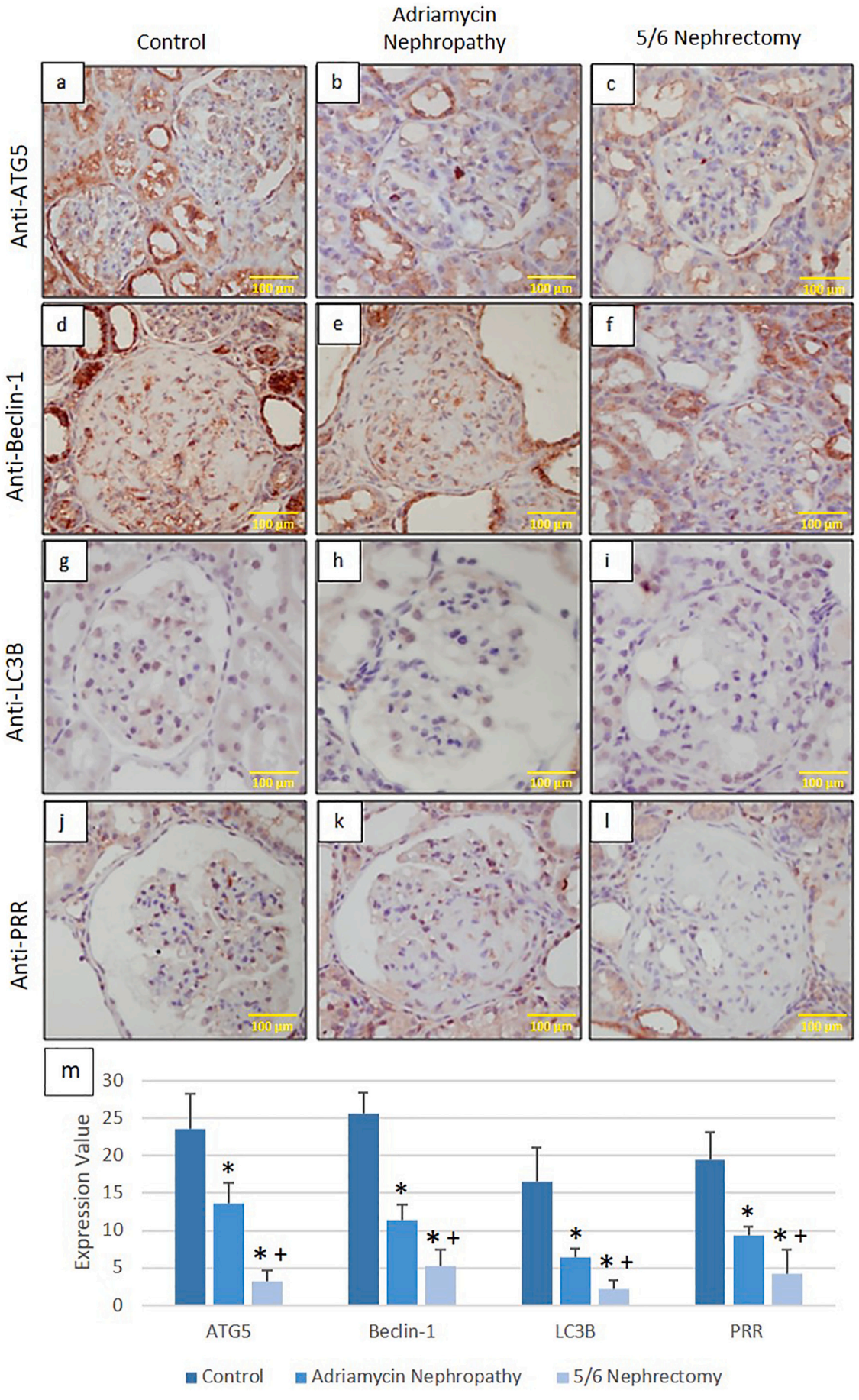

(caption on next page)

Fig. 3. Immunohistochemical findings performed with Anti-ATG5, Anti-Beclin-1, Anti LC3B and Anti-PRR antibodies in FSGS and control groups. IM ×400 magnification. a, b, c: Anti-ATG5; d, e, f: Beclin; g, h, i: LC3B; j, k, l: PRR antibody; a, d, g, j: Control group; b, e, h, k: adriamycin induced nephropathy and c, f, i, l: 5/6 nephrectomy group. m: Quantification of expression. *Significantly different from control group ($p < 0.01$). $^{+}$Significantly different from adriamycin nephropathy group ($p < 0.05$).

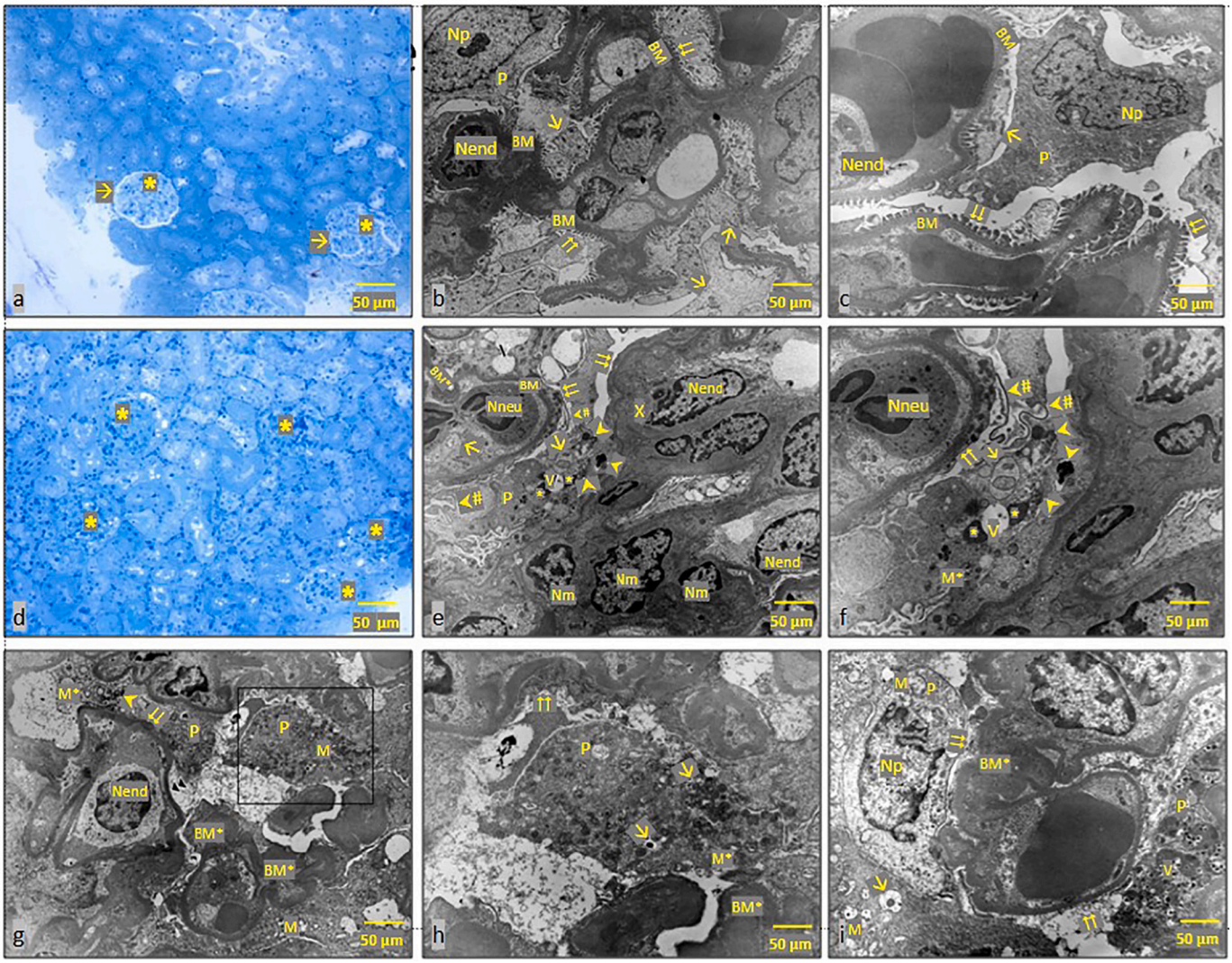

Fig. 4. Electron microscopic examination of the glomerular structures of the renal cortex in the control group and 5/6 nephrectomy. a: Control group: Semi-thin section, ✱; Glomeruli, →; Urinary space. (Toluidine BlueX400). b: Control Group: Thin Section: P; Podocyte, Np; Podocyte nucleus, →; Podocyte primary extension, ⇉; Pedisel, Nend; Endothelial nucleus, BM; basal membrane (Uranyl Acetate & Lead Citrate X2186). c: Control Group: Thin Section: P; Podocyte, Np; Podocyte nucleus, →; Podocyte primary extension, ⇉; Pedisel, Nend; Endothelial nucleus, BM; basement membrane (Uranyl Acetate & Lead Citrate X4646). d: 5/6 nephrectomy: Semi-thin section; ✱; Sclerotic glomeruli (Toluidine BlueX 400). e: 5/6 nephrectomy: Thin Section: P; Podocyte, ⇉; Fusion in pedicels, #➤; Thinning in podocyte extensions, Nend; Endothelial nucleus, Nm: Mesengial cell nucleus, Nneu; Neutrophil nucleus, ➤; Degenerate cell debris cluster, →; Autophagic vacuole, V; Vacuole, ✱; electron dense oval bodies, X: Subendothelial deposition, BM; basal membrane, BM*; Thickening of the basement membrane (Uranyl Acetate & Lead Citrate X2784). f: 5/6 nephrectomy: Thin Section: ⇉; Fusion in pedicels, #➤; Thinning in podocyte extensions, Nneu; Neutrophil nucleus, ➤; Degenerate cell debris cluster, →; Autophagic vacuole, V; Vakuol, M*; degenerate mitochondria, ✱; electron dense oval bodies (Uranyl Acetate & Lead Citrate X4646). g: 5/6 nephrectomy: Thin Section: P; Podocyte, ⇉; Fusion in pedicels, Nend; Endothelial nucleus, ➤; Degenerate cell debris cluster, M*; degenerate mitochondria, BM*; Thickening of the basement membrane (Uranyl Acetate & Lead Citrate X2784). h: 5/6 nephrectomy: Thin Section: Higher magnification of the square area in panel g P; Podocytes, ⇉; Fusion in pediceles, M*; degenerate mitochondria, →; Autophagic vacuole, BM*; Thickening of basement membrane (Uranyl Acetate & Lead Citrate X6000). i: 5/6 nephrectomy: Thin Section: P; Podocyte, P*; podocytes with apoptotic objects, Np; Podocyte nucleus, ⇉; Fusion in pediceles, M*; degenerate mitochondria, →; Autophagic vacuole, BM*; Thickening of the basement membrane (Uranyl Acetate & Lead Citrate X4646).

renal diseases like urinary miR-196a in disease progression of chronic kidney disease [42]; urinary miRNAs 10a and 30d for kidney injury [43]; miRNAs 17, 451,106a and 19b as biomarkers of FSGS [14]; miRNAs 34b, 34c, 342,12255p, 1915 and 663 for minimal change of disease and FSGS [13]. It has been reported that miR-30 expression is down-regulated in the podocytes of FSGS patients, glucocorticoid therapy maintains miR-30 levels and may have a role in treatment effectiveness [44]. Transgenic expression of miR-193a in mice ended with FSGS by inhibiting Wilms Tumor Protein-1 expression, an important regulator of podocyte differentiation and homeostasis [45].

In our study; mi-R34c, miR-132 and miR-214 increased among the transcripts identified by microarray examination to determine key

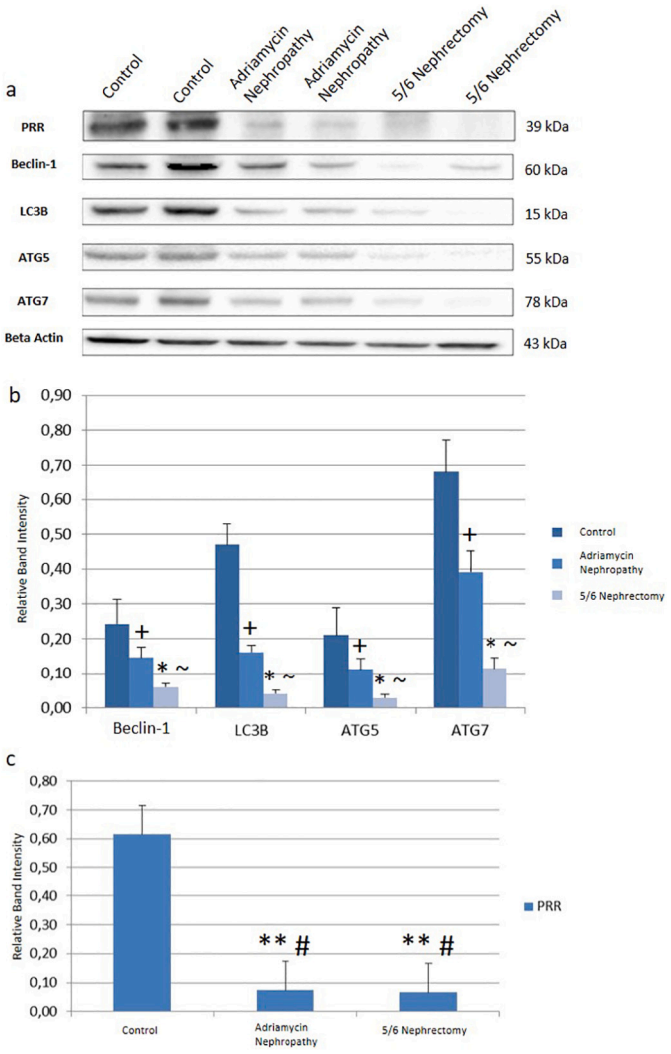

Fig. 5. Protein expression levels of PRR and autophagic markers Beclin-1, LC3B, ATG5, ATG7 in FSGS and control groups. 5.a. Band images of western blot results of samples studied in duplicate 5.b. Normalized expression values of Western Blot study performed with anti-Beclin-1, Anti-LC3B, Anti-ATG5 and Anti-ATG7 antibodies in models and control groups. Data are representative of three (n = 3) independent experiments and values are expressed in mean ± SEM for all groups. *Significantly different from control group ($p < 0.01$). $^{+}$Significantly different from control group ($p < 0.05$). $^{\sim}$Significantly different from Adriamycin nephropathy group ($p < 0.05$). 5.c. Normalized expression values of Western Blot study performed with anti-PRR antibody in models and control groups. Data are representative of three (n = 3) independent experiments and values are expressed in mean ± SEM for all groups. **Significantly different from control group ($p < 0.001$). $^{\#}$No significant difference between Adriamycin Nephropathy and 5/6 Nephrectomy groups ($p > 0.05$).

miRNA molecules in FSGS. Among these, an article related to miR34c reported the association of miR34c with autophagy in the tumor microenvironment in cancer cells [46]. miR-214 is expressed at high levels in human and animal models of kidney disease [47] which promotes chronic kidney disease by disrupting mitochondrial oxidative phosphorylation [48]. miRNA-214 has also been included in a recent meta-analysis as one of upregulated genes with renal fibrosis [49]. miR-214 is cotranscribed with the miR-199a family on a single lncRNA strand located on the complementary strand of an intron in the dynamin-3 gene. miR-214 and miR-199a are upregulated by activation of the TWIST transcription factor and by hypoxia via HIF-1α. In kidney samples obtained from patients with various kidney diseases, miR-214 was detected in renal tubules, glomeruli, and infiltrating immune cells [50]. In the mouse unilateral ureteric obstruction model, decreased expression of miR-214 protected against the development of fibrosis, and treatment of WT mice with anti-miR-214 before UUO resulted in similar antifibrotic effects [50,51].

miR-34c was also associated with many other conditions like cancer development, metastasis and embryonic processes [52–54]. Also, this molecule was showed important relationship with renal diseases. In a rat model, it is showed that miR-34c is upregulated at acute contrast induced renal injury [55]. Administration of miR-34c in a mouse model of unilateral ureteral obstruction attenuated kidney fibrosis and expression of fibrosis markers [56]. In another study miR-34c levels were found significantly higher in minimal change disease but not in FSGS when compared to controls [13]. In a study, aldosterone-induced downregulation of miR-34c-5p in the Wnt signaling and the consequent increase in CaMKIIβ expression played a role in aldosterone-induced fibrosis [57]. Also an article suggest that miR-34c overexpression inhibits the Notch signaling pathway by targeting Notch1 and Jaggged1 in HG-treated podocytes, representing a novel and potential therapeutic target for the treatment of diabetic nephropathy [58].

miR-132 was also associated with many conditions like cerebral hypoperfusion and tuberous sclerosis complex [59,60]. Recently, miR-132 and miR-212 were reported to be increased in the heart, aorta, and kidney of ANG II-induced hypertensive rats and decreased in human arteries obtained from patients undergoing bypass surgery, in response to ANG II type 1 receptor (AT1) blockade [61]. In light of evidence that MMP-9 is a target of miR-132 [62], the role of MMP-9 in mediating the effect of miR132 on renal fibrosis warrants additional consideration [51].

In our study, literature was reviewed and we focused on a total of 12 miRNAs that may play a role in the pathogenesis and autophagy regulation of FSGS; miR-212, miR-132, miR-21, miR-146b, miR-130b, miR-34a, miR-34c, miR-18a, miR-376b-3p, miR-214, miR-192 and miR-29c and quantitative real-time PCR verification was performed . Specifically, we planned to study mimic and antagonists of miRNAs on detection of increased expression of miR-132 in patient groups about 7 and 11-fold, miR-34c approximately 3 and 11-fold, and miR-214 approximately 8 and 13-fold. Autophagic activity was evaluated after transfection with the miR-34c, miR-132 and miR-214 mimic and post-transfection with miR-34c, miR-132 and miR-214 antagonists in podocytes of rat kidney tissues. We showed decrease in marker levels showing autophagic activity when mimics of miR-34c, 132 and 214 were applied and increase in autophagy markers when antagonists of these miRNAs were transfected. Our study is an important report which supporting the studies showing that autophagy is a protective factor in FSGS, as well as identifying specific miRNAs that are important in the pathogenesis of FSGS and their relationship with autophagic activity and the possible location of treatment.

PRR is a newly defined member of the renin-angiotensinogen system and has been found to have independent effects on blood pressure regulation and renin angiotensinogen system in recent years [63–65]. It has been reported that RAS activation plays a role in mesangial expansion in IgAN model mice because administration of an angiotensin II type1 receptor blocker ameliorated the extent of mesangial matrix expansion [66]. PRR deletion was performed in podocytes in some studies and knock-out mice developed proteinuria and glomerulosclerosis characterized by renal failure [67,68]. The inhibition of PRR or ERK1/2 signaling attenuated mesangial expansion and decreased the expression of fibrotic factors [66–69]. This is very similar to that observed by Kinouchi et al. in PRR knockout cardiomyocytes [70]. In another study examined the correlation between serum soluble PRR and various laboratory data including serum indoxyl sulphate (IS) and pathological indices in chronic kidney disease and particularly in IgA nephropathy patients. They revealed that PRR expression significantly increased in the presence of IS [23]. Studies supporting the relationship between PRR and mesengial fibrosis have suggested that this molecule may also be important in the pathogenesis of FSGS [71,72]. In our study,

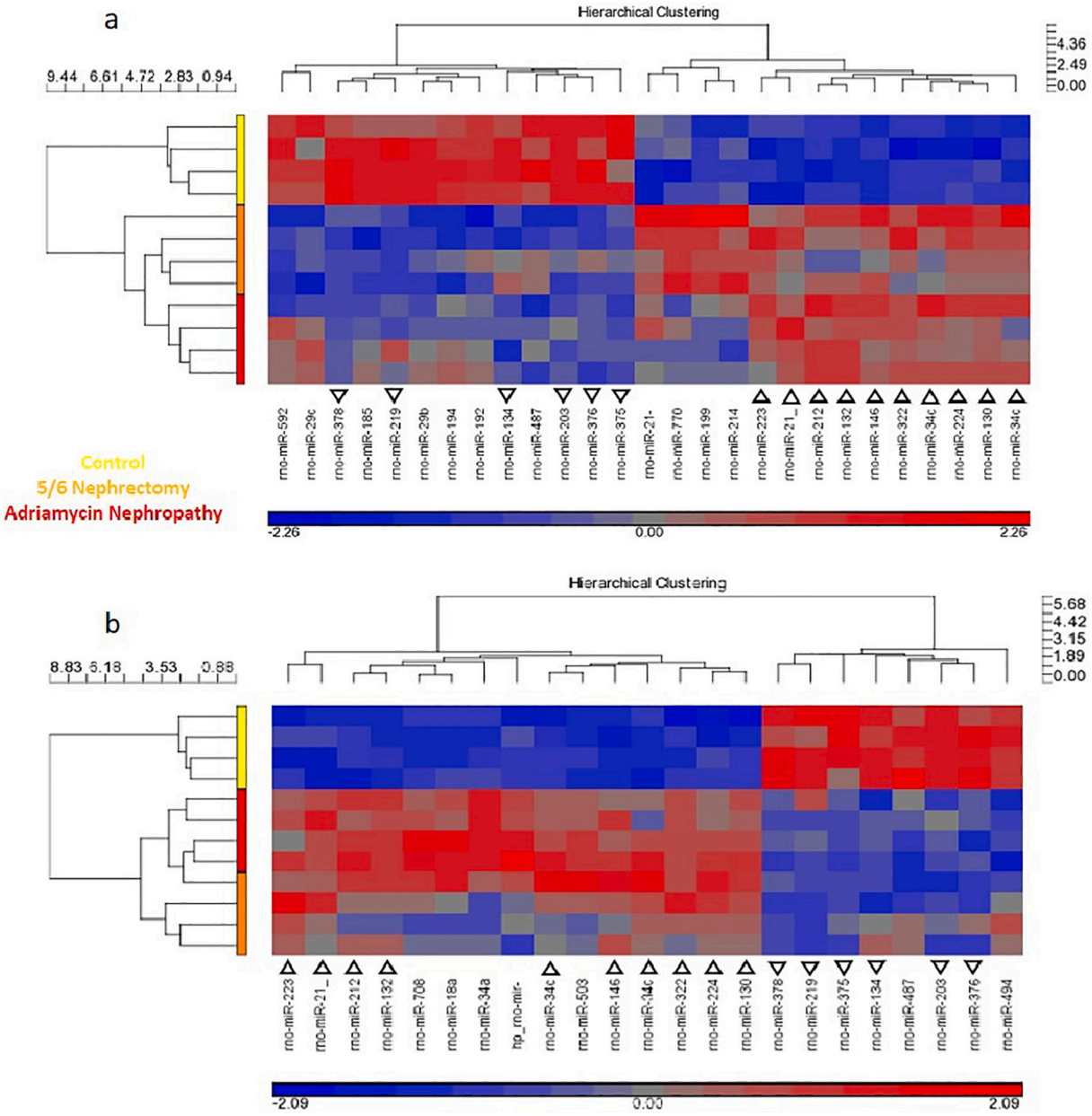

Fig. 6. Heatmap representation of differantially expressed miRNA profiling of FSGS and control groups (n = 4 per group). a. Heatmap of hierarchical clustering showing 27 miRNAs significantly regulated which were 15 miRNAs upregulated and 8 miRNAs downregulated in 5/6 nephrectomy group, compared to the control group. b. In Adriamycin group 23 significantly regulated miRNAs which were 15 miRNAs upregulated and 8 miRNAs downregulated compared to the control group. △ Common upregulated miRNAs in both experimental groups. ▽ Common downregulated miRNAs in both experimental groups.

we have demonstrated that PRR is decreased in primary and secondary FSGS when compared to healthy rats. Also, we have shown that primary FSGS has lower PRR levels than secondary form.

Activation of the RAAS system is one of the important causes of renal diseases, especially chronic kidney diseases. Enzyme inhibitors or receptor blockers are used against these system components in the clinic. Although it is desired to reduce the progression of the disease with such inhibition strategies, more effective treatment agents or modulators are investigated [73]. miRNAs come to the fore with their potent modulator functions on signaling networks in metabolism. Detecting miRNAs expression levels makes a great contribution to the determination of specific disease targets. In addition, they are effective agents in both early diagnosis and the development of new treatment combinations. Molecular modeling and meta-analysis methods are frequently used to locate miRNAs in complex signaling networks. In a prediction study by Agarval et al. 368 different miRNAs targeting RAS system elements were identified [74,75]. This study reveals the importance of the experimental approach to miRNA-RAAS relationship. However, experimental studies of miRNAs that interact with RAAS targets are limited. miRNAs 34c, 132 and 212, which were shown to be effective on FSGS in our study, were also reported to be associated with some RAAS family members. In a study investigating any miRNAs targeting placental RAS in human placenta, miR-34c, predicted to target AGTR1 (also known as AT1R) mRNA from RAS family, was found to be differentially expressed with a − 91.2-fold [76]. Also, AGTR1 is one of the target genes of FSGS from GeneCards database [77]. In another study, miR-34c was expressed significantly different levels in normal adrenal and aldosterone-producing adenoma tissues and was predicted to bind both the CYP11B1 (11β-hydroxylase) and the CYP11B2 (aldosterone synthase) [78]. Here, considering the known relationship of AGTR1 with chronic

Table 2
q-RT-PCR Verification of FSGS-related miRNAs. miR-34, miR-132 and miR-214 have been determined the most upregulated miRNAs (n = 4 per group).

	Fold change (Relative to control)	
	Adriamycin group	5/6 nephrectomy group
Control	1	1
miR-212	1.2924	2.1886
miR-34c	3.2944	11.8762
miR-21	3.5064	5.4453
miR-132	7.2854	10.8528
miR-146	1.8404	8.1965
miR-130b	1.4673	4.9652
miR-34a	2.2471	2.4665
miR-18a	4.6631	3.5791
miR-376b	1.3848	1.9654
miR-214	8.5243	12.968
miR-192	2.4576	2.1977
miR-29c	5.4885	3.2733

kidney diseases, the findings obtained from our study showed a correlation with miR-34c and RAAS [79,80]. When the relationship between miR-132 and RAAS targets was investigated, a tightly regulated phenotype was found between miR-132 and AngII (Angiotensin II) [81]. Jeppesen et al. found that miR-132 expression was significantly and directly upregulated in Ang II treated AT1R-HEK (AT1R-expressed human embryonic kidney) cells via Gaq and Erk1/2 [82]. In another functional study, an increase in miR-132 expression was observed in different tissues (heart, aortic wall, and kidney) of AngII-induced hypertension model rats. In the same study, it was observed that miR-212 expression level was decreased in arterial samples of patients who used various AT1R blockers [61]. A recent study revealed the direct roles of miR-132 in the mechanism of body fluid and salt balance under the RAAS regulation. It has been reported that miR-132 affects PGE2 (prostaglandin-E2) and Renin levels by targeting COX-2 (cyclo-oxygenase-2) in macula densa kidney cells in mice. Also, this equation was verified in various salt diets with mode-of-action experiments [83]. Due to the expression of AT1Rs in podocytes and their functional roles, modulation by miR-132 is also critical for FSGS. Since the studies have reported podocyte damage and various renal pathologies due to AT1R activation, it is very critical that the efficacy of miR-132 on FSGS was determined as a result of our study [84]. The evidence for miR-214 relationship with RAAS targets is more limited than others. Liu et al. investigated many rat RAS genes for possible targets against miR-124 but found no relationship other than a minor Ace transcript [85]. In another study, miR-214 also increased 8-fold in the mouse model of AngII-mediated hypertension [86].

Our study elucidated the role of autophagy in pathogenesis of FSGS. If miRNA antagonists would be commonly used in treatment of disease, progression and percentage of end stage renal disease may be reduced. There are many ongoing clinical phase trial studies on miRNA molecules. We think that our study has value in two different aspects. First, as understanding the molecular basis of diseases is very critical on the road to therapy, it enlightened the concept of autophagy/miRNA with FSGS. Secondly, with the data sets obtained here, it can be applied to all other disciplines. However, although our study provides strong evidence with molecular methods that validate each other with different results in unique animal models, there are some limitations. The most important of these is the resolution of miRNA profiling. Next generation sequencing-based RNA profiling can give sharper and more precise

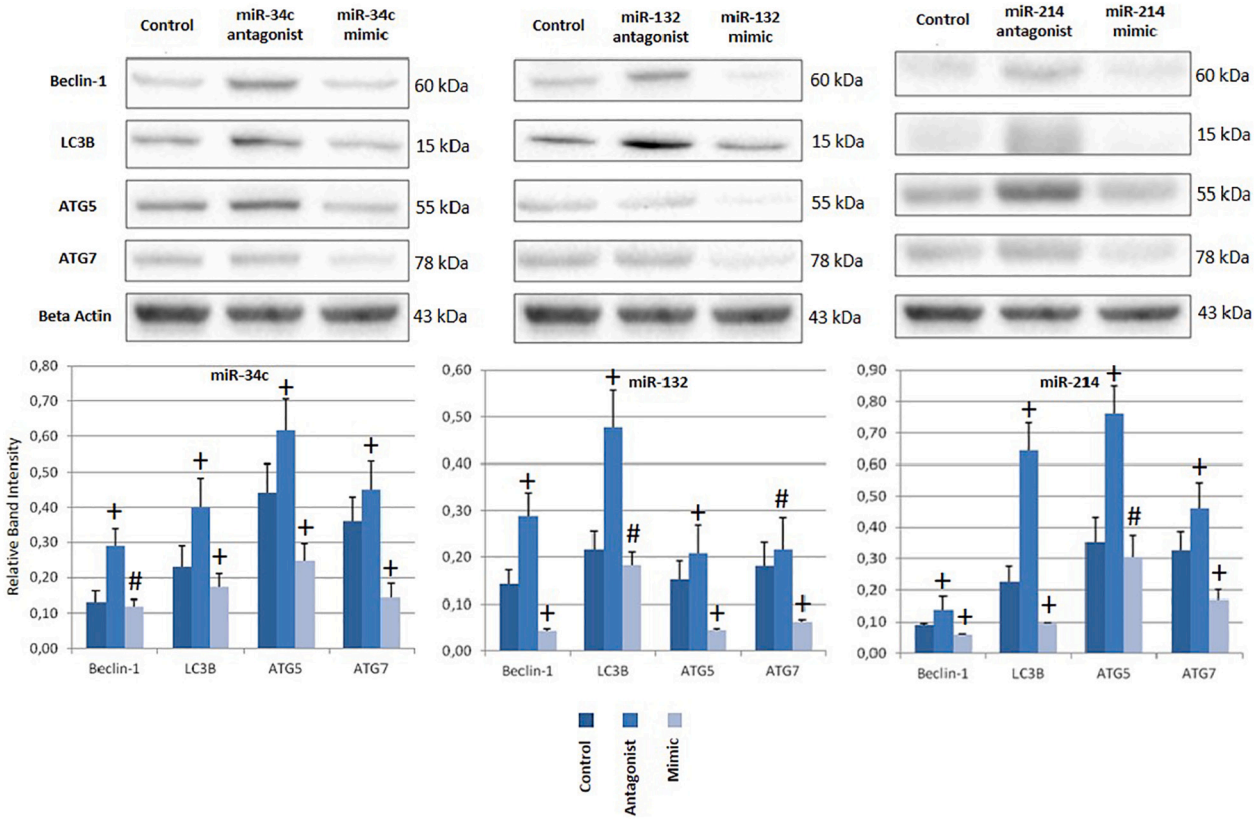

Fig. 7. Evaluation of the effects of selected intrarenal miRNAs on autophagic markers in primary podocyte cells isolated from 5/6 nephrectomy model rats. Beclin-1, L3CB, ATG5 and ATG7 protein expression levels were evaluated after transfections of mimics and antagonists of 3 miRNAs onto podocytes. Normalized densitometric analysis of each western blot run is plotted below the protein band images. Left panel: miR-34c, Middle panel: miR-132, Right panel: miR-214. Data are representative of three (n = 3) independent experiments and values are expressed in mean ± SEM for all groups. $^{+}$Significantly different from control group ($p < 0.05$). $^{\#}$No significant difference between the experimental and control group ($p > 0.05$).

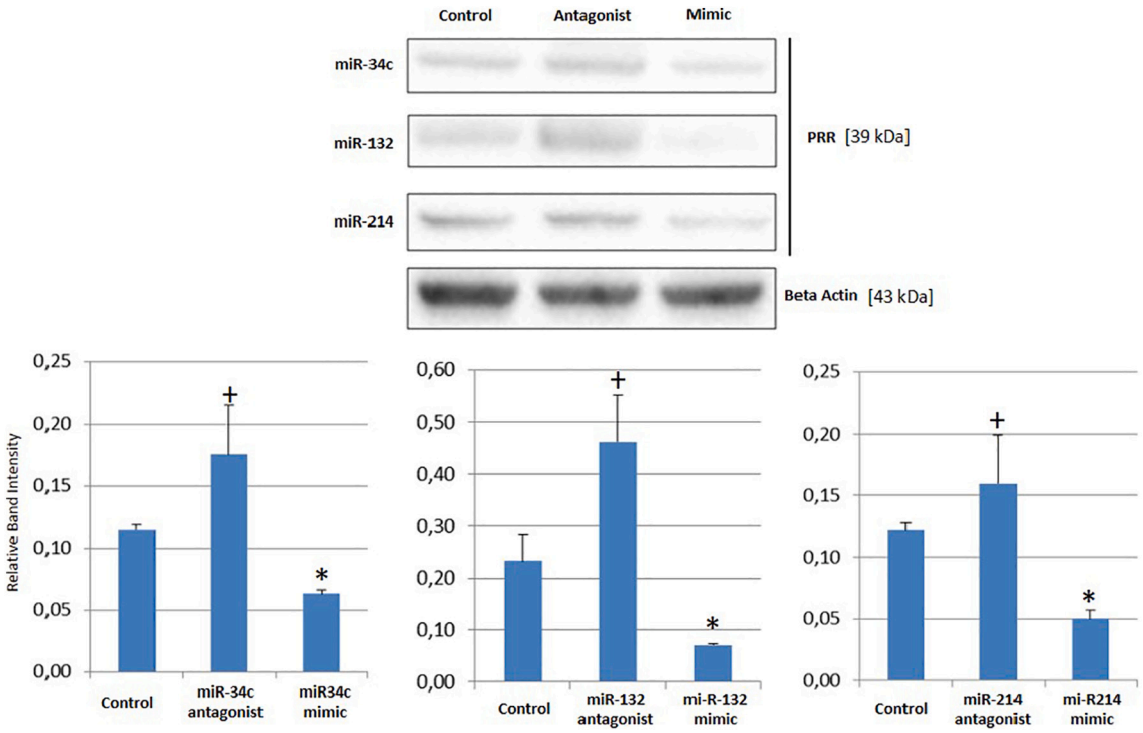

Fig. 8. Evaluation of the effects of selected intrarenal miRNAs on PRR in primary podocyte cells isolated from 5/6 nephrectomy model rats. PRR protein expression levels were evaluated after transfections of mimics and antagonists of 3 miRNAs onto podocytes. Normalized densitometric analysis is plotted below the protein band images. Data are representative of three (n = 3) independent experiments and values are expressed in mean ± SEM for all groups. *Significantly different from control group ($p < 0.01$). $^{+}$Significantly different from control group ($p < 0.05$).

results. In addition, the correlation between the identified miRNAs and the expression levels in FSGS patient samples could be determined. These limitations can be overcome by high technology-based studies based on the data of our study. Also, determination of possible activities that may occur with in vivo treatments of selected miRNA mimics and antagonists can be listed among the limitations. But the integration and efficiency of this type of work into the transport systems is one of the ongoing problems for years. However, this is mostly possible with applications that can be overcome with materials science and engineering. Collaboration with different disciplines is required.

5. Conclusions

This is the first study about the relationship between PRR and FSGS. Here we shed light on the molecular pathogenesis of glomerular damage caused by dysregulation of specific miRNAs. Our results may elucidate the unknown roles of these miRNAs by suggesting that miR-34c, miR-132 and miR-214 play a role in autophagy regulation and PRR expression in podocytes by regulating the expression of key autophagy proteins, and these sizes show a potential treatment agent in the prognosis of podocytopenias. The pathogenesis of pathological miRNA expression increases is still unclear. Further trials are needed on this subject.

Funding

This work was supported The Scientific and Technological Research Council of Turkey (TUBITAK) [grant number: 112S253].

CRediT authorship contribution statement

All authors contributed to the study conception and design. DY, OB, ZFK, FH and NBR performed experiments and analyzed experimental data. MAB, AA and NBR provided critical advice during the study. The first draft of the manuscript was written by DY, OB and NBR. All authors read and approved the final manuscript.

Declaration of competing interest

The authors declare that there are no conflicts of interest.

References

[1] W. Lieberthal, Macroautophagy: a mechanism for mediating cell death or for promoting cell survival? Kidney Int. 74 (2008) 555–557.
[2] T. Kawakami, I.G. Gomez, S. Ren, K. Hudkins, A. Roach, C.E. Alpers, S. J. Shankland, V.D. D'Agati, J.S. Duffield, Deficient autophagy results in mitochondrial dysfunction and FSGS, J. Am. Soc. Nephrol. 26 (2015) 1040–1052.
[3] S. Vasudevan, Y. Tong, J.A. Steitz, Switching from repression to activation: microRNAs can up-regulate translation, Science 318 (2007) 1931–1934 (80-.).
[4] P.S. Mitchell, R.K. Parkin, E.M. Kroh, B.R. Fritz, S.K. Wyman, E.L. Pogosova-Agadjanyan, A. Peterson, J. Noteboom, K.C. O'Briant, A. Allen, Circulating microRNAs as stable blood-based markers for cancer detection, Proc. Natl. Acad. Sci. 105 (2008) 10513–10518.
[5] M.A. Cortez, C. Bueso-Ramos, J. Ferdin, G. Lopez-Berestein, A.K. Sood, G.A. Calin, MicroRNAs in body fluids—the mix of hormones and biomarkers, Nat. Rev. Clin. Oncol. 8 (2011) 467.
[6] X.-J. Lin, Y. Chong, Z.-W. Guo, C. Xie, X.-J. Yang, Q. Zhang, S.-P. Li, Y. Xiong, Y. Yuan, J. Min, A serum microRNA classifier for early detection of hepatocellular carcinoma: a multicentre, retrospective, longitudinal biomarker identification study with a nested case-control study, Lancet Oncol. 16 (2015) 804–815.
[7] V.R. Mas, C.I. Dumur, M.J. Scian, R.C. Gehrau, D.G. Maluf, MicroRNAs as biomarkers in solid organ transplantation, Am. J. Transplant. 13 (2013) 11–19.
[8] V.K. Nagalakshmi, Q. Ren, M.M. Pugh, M.T. Valerius, A.P. McMahon, J. Yu, Dicer regulates the development of nephrogenic and ureteric compartments in the mammalian kidney, Kidney Int. 79 (2011) 317–330.
[9] A.K. Marrone, D.B. Stolz, S.I. Bastacky, D. Kostka, A.J. Bodnar, J. Ho, MicroRNA-17~92 is required for nephrogenesis and renal function, J. Am. Soc. Nephrol. 25 (2014) 1440–1452.
[10] C.-L. Lin, P.-H. Lee, Y.-C. Hsu, C.-C. Lei, J.-Y. Ko, P.-C. Chuang, Y.-T. Huang, S.-Y. Wang, S.-L. Wu, Y.-S. Chen, MicroRNA-29a promotion of nephrin acetylation ameliorates hyperglycemia-induced podocyte dysfunction, J. Am. Soc. Nephrol. 25 (2014) 1698–1709.
[11] V. Patel, D. Williams, S. Hajarnis, R. Hunter, M. Pontoglio, S. Somlo, P. Igarashi, miR-17~92 miRNA cluster promotes kidney cyst growth in polycystic kidney disease, Proc. Natl. Acad. Sci. 110 (2013) 10765–10770.

[12] H. Zhou, S.A. Hasni, P. Perez, M. Tandon, S.-I. Jang, C. Zheng, J.B. Kopp, H. Austin, J.E. Balow, I. Alevizos, miR-150 promotes renal fibrosis in lupus nephritis by downregulating SOCS1, J. Am. Soc. Nephrol. 24 (2013) 1073–1087.

[13] A. Ramezani, J.M. Devaney, S. Cohen, M.R. Wing, R. Scott, S. Knoblach, R. Singhal, L. Howard, J.B. Kopp, D.S. Raj, Circulating and urinary micro RNA profile in focal segmental glomerulosclerosis: a pilot study, Eur. J. Clin. Investig. 45 (2015) 394–404.

[14] B. Xiao, L.-N. Wang, W. Li, L. Gong, T. Yu, Q.-F. Zuo, H.-W. Zhao, Q.-M. Zou, Plasma microRNA panel is a novel biomarker for focal segmental glomerulosclerosis and associated with podocyte apoptosis, Cell Death Dis. 9 (2018) 1–14.

[15] S. Satofuka, A. Ichihara, N. Nagai, K. Noda, Y. Ozawa, A. Fukamizu, K. Tsubota, H. Itoh, Y. Oike, S. Ishida, (Pro) renin receptor–mediated signal transduction and tissue renin-angiotensin system contribute to diabetes-induced retinal inflammation, Diabetes 58 (2009) 1625–1633.

[16] A. Arundhathi, W.-H. Chuang, J.-K. Chen, S.-E. Wang, Y.-M. Shyr, J.-Y. Chen, W.-N. Liao, H.-W. Chen, Y.-M. Teng, C.-C. Pai, Prorenin receptor acts as a potential molecular target for pancreatic ductal adenocarcinoma diagnosis, Oncotarget 7 (2016), 55437.

[17] K. Hamada, Y. Taniguchi, Y. Shimamura, K. Inoue, K. Ogata, M. Ishihara, T. Horino, S. Fujimoto, T. Ohguro, Y. Yoshimoto, Serum level of soluble (pro) renin receptor is modulated in chronic kidney disease, Clin. Exp. Nephrol. 17 (2013) 848–856.

[18] P. Tan, Z. Shamansurova, S. Bisotto, C. Michel, M. Gauthier, R. Rabasa-Lhoret, T. M. Nguyen, P.W. Schiller, J. Gutkowska, J.L. Lavoie, Impact of the prorenin/renin receptor on the development of obesity and associated cardiometabolic risk factors, Obesity 22 (2014) 2201–2209.

[19] J. Thomason, M. Reyes, S.R. Allen, R.O. Jones, M.R. Beeram, T.J. Kuehl, F. Suzuki, M.N. Uddin, Elevation of (pro) renin and (pro) renin receptor in preeclampsia, Am. J. Hypertens. 28 (2015) 1277–1284.

[20] K. Hase, A. Kanda, I. Hirose, K. Noda, S. Ishida, Systemic factors related to soluble (pro) renin receptor in plasma of patients with proliferative diabetic retinopathy, PLoS One 12 (2017), e0189696.

[21] I.V. Yosypiv, M.L.S. Sequeira-Lopez, R. Song, A. De Goes Martini, Stromal prorenin receptor is critical for normal kidney development, Am. J. Physiol. Integr. Comp. Physiol. 316 (2019) R640–R650.

[22] K. Narumi, T. Hirose, E. Sato, T. Mori, K. Kisu, M. Ishikawa, K. Totsune, T. Ishii, A. Ichihara, G. Nguyen, A functional (pro) renin receptor is expressed in human lymphocytes and monocytes, Am. J. Physiol. Physiol. 308 (2015) F487–F499.

[23] K. Narumi, E. Sato, T. Hirose, T. Yamamoto, T. Nakamichi, M. Miyazaki, H. Sato, S. Ito, (Pro) renin receptor is involved in mesangial fibrosis and matrix expansion, Sci. Rep. 8 (2018) 1–11.

[24] T. Bertani, G. Rocchi, G. Sacchi, G. Mecca, G. Remuzzi, Adriamycin-induced glomerulosclerosis in the rat, Am. J. Kidney Dis. 7 (1986) 12–19.

[25] M.L. Purkerson, P.E. Hoffsten, S. Klahr, Pathogenesis of the glomerulopathy associated with renal infarction in rats, Kidney Int. 9 (1976) 407–417.

[26] S.S. Amarasiri, A.P. Attanayake, L.D.A.M. Arawwawala, K.A.P.W. Jayatilaka, L.K. B. Mudduwa, Protective effects of three selected standardized medicinal plant extracts used in Sri Lankan traditional medicine in adriamycin induced nephrotoxic Wistar rats, J. Ethnopharmacol. 259 (2020), 112933.

[27] S. He, A. Li, W. Zhang, L. Zhang, Y. Liu, K. Li, X. Qin, An integrated transcriptomics and network pharmacology approach to exploring the mechanism of adriamycin-induced kidney injury, Chem. Biol. Interact. 325 (2020), 109096.

[28] Y. Wang, T. Zhang, X. Cao, J. Zou, X. Ding, B. Shen, W. Lv, Prostaglandin E2 induced cardiac hypertrophy through EP2 receptor-dependent activation of β-catenin in 5/6 nephrectomy rats, ESC Hear. Fail. 8 (2021) 1979–1989.

[29] S.H. Son, S.M. Lee, M.H. Lee, Y.K. Son, S.E. Kim, W.S. An, Omega-3 fatty acids upregulate SIRT1/3, activate PGC-1α via deacetylation, and induce Nrf1 production in 5/6 nephrectomy rat model, Mar. Drugs 19 (2021) 182.

[30] V.W.S. Lee, D.C.H. Harris, Adriamycin nephropathy: a model of focal segmental glomerulosclerosis, Nephrology 16 (2011) 30–38.

[31] A.B. Fogo, Causes and pathogenesis of focal segmental glomerulosclerosis, Nat. Rev. Nephrol. 11 (2015) 76–87.

[32] B. Hartleben, N. Wanner, T.B. Huber, Autophagy in glomerular health and disease, in: Semin. Nephrol, Elsevier, 2014, pp. 42–52.

[33] B. Hartleben, M. Gödel, C. Meyer-Schwesinger, S. Liu, T. Ulrich, S. Köbler, T. Wiech, F. Grahammer, S.J. Arnold, M.T. Lindenmeyer, Autophagy influences glomerular disease susceptibility and maintains podocyte homeostasis in aging mice, J. Clin. Invest. 120 (2010) 1084–1096.

[34] E.F. Carney, Autophagy failure and mitochondrial dysfunction in FSGS, Nat. Rev. Nephrol. 11 (2015) 66.

[35] V. Ghai, D. Baxter, X. Wu, T. Kim, J. Kuusisto, M. Laakso, T. Connolly, Y. Li, P. Andrade-Gordon, K. Wang, Circulating RNAs as predictive markers for the progression of type 2 diabetes, J. Cell. Mol. Med. 23 (2019) 2753–2768.

[36] J. Xiao, R. Gao, Y. Bei, Q. Zhou, Y. Zhou, H. Zhang, M. Jin, S. Wei, K. Wang, X. Xu, Circulating miR-30d predicts survival in patients with acute heart failure, Cell. Physiol. Biochem. 41 (2017) 865–874.

[37] V. Ghai, K. Wang, Recent progress toward the use of circulating microRNAs as clinical biomarkers, Arch. Toxicol. 90 (2016) 2959–2978.

[38] V. Patel, S. Hajarnis, D. Williams, R. Hunter, D. Huynh, P. Igarashi, MicroRNAs regulate renal tubule maturation through modulation of Pkd1, J. Am. Soc. Nephrol. 23 (2012) 1941–1948.

[39] L. Liu, X.-L. Pang, W.-J. Shang, H.-C. Xie, J.-X. Wang, G.-W. Feng, Over-expressed microRNA-181a reduces glomerular sclerosis and renal tubular epithelial injury in rats with chronic kidney disease via down-regulation of the TLR/NF-κB pathway by binding to CRY1, Mol. Med. 24 (2018) 1–14.

[40] F.P. Schena, F. Sallustio, G. Serino, microRNAs in glomerular diseases from pathophysiology to potential treatment target, Clin. Sci. 128 (2015) 775–788.

[41] P. Trionfini, A. Benigni, G. Remuzzi, MicroRNAs in kidney physiology and disease, Nat. Rev. Nephrol. 11 (2015) 23.

[42] C. Zhang, S. Liang, S. Cheng, W. Li, X. Wang, C. Zheng, C. Zeng, S. Shi, L. Xie, K. Zen, Urinary miR-196a predicts disease progression in patients with chronic kidney disease, J. Transl. Med. 16 (2018), 91.

[43] N. Wang, Y. Zhou, L. Jiang, D. Li, J. Yang, C.-Y. Zhang, K. Zen, Urinary microRNA-10a and microRNA-30d serve as novel, sensitive and specific biomarkers for kidney injury, PLoS One 7 (2012) e51140.

[44] J. Wu, C. Zheng, Y. Fan, C. Zeng, Z. Chen, W. Qin, C. Zhang, W. Zhang, X. Wang, X. Zhu, Downregulation of microRNA-30 facilitates podocyte injury and is prevented by glucocorticoids, J. Am. Soc. Nephrol. 25 (2014) 92–104.

[45] C.A. Gebeshuber, C. Kornauth, L. Dong, R. Sierig, J. Seibler, M. Reiss, S. Tauber, M. Bilban, S. Wang, R. Kain, Focal segmental glomerulosclerosis is induced by microRNA-193a and its downregulation of WT1, Nat. Med. 19 (2013) 481–487.

[46] S. Pavlides, A. Tsirigos, G. Migneco, D. Whitaker-Menezes, B. Chiavarina, N. Flomenberg, P.G. Frank, M.C. Casimiro, C. Wang, R.G. Pestell, The autophagic tumor stroma model of cancer: role of oxidative stress and ketone production in fueling tumor cell metabolism, Cell Cycle 9 (2010) 3485–3505.

[47] I.G. Gomez, N. Nakagawa, J.S. Duffield, MicroRNAs as novel therapeutic targets to treat kidney injury and fibrosis, Am. J. Physiol. Physiol. 310 (2016) F931–F944.

[48] M. Bai, H. Chen, D. Ding, R. Song, J. Lin, Y. Zhang, Y. Guo, S. Chen, G. Ding, Y. Zhang, MicroRNA-214 promotes chronic kidney disease by disrupting mitochondrial oxidative phosphorylation, Kidney Int. 95 (2019) 1389–1404.

[49] A. Gholaminejad, H. Abdul Tehrani, M. Gholami Fesharaki, Identification of candidate microRNA biomarkers in renal fibrosis: a meta-analysis of profiling studies, Biomarkers 23 (2018) 713–724.

[50] L. Denby, V. Ramdas, R. Lu, B.R. Conway, J.S. Grant, B. Dickinson, A.B. Aurora, J. D. McClure, D. Kipgen, C. Delles, MicroRNA-214 antagonism protects against renal fibrosis, J. Am. Soc. Nephrol. 25 (2014) 65–80.

[51] W. Lv, F. Fan, Y. Wang, E. Gonzalez-Fernandez, C. Wang, L. Yang, G.W. Booz, R. J. Roman, Therapeutic potential of microRNAs for the treatment of renal fibrosis and CKD, Physiol. Genomics 50 (2018) 20–34.

[52] Z. Hagman, O. Larne, A. Edsjö, A. Bjartell, R.A. Ehrnström, D. Ulmert, H. Lilja, Y. Ceder, miR-34c is downregulated in prostate cancer and exerts tumor suppressive functions, Int. J. Cancer 127 (2010) 2768–2776.

[53] C. Migliore, A. Petrelli, E. Ghiso, S. Corso, L. Capparuccia, A. Eramo, P. M. Comoglio, S. Giordano, MicroRNAs impair MET-mediated invasive growth, Cancer Res. 68 (2008) 10128–10136.

[54] X. Liang, D. Zhou, C. Wei, H. Luo, J. Liu, R. Fu, S. Cui, MicroRNA-34c enhances murine male germ cell apoptosis through targeting ATF1, PLoS One 7 (2012) e33861.

[55] Y. Liu, B. Liu, Y. Liu, S. Chen, J. Yang, J. Liu, G. Sun, W.-J. Bei, K. Wang, Z. Chen, MicroRNA expression profile by next-generation sequencing in a novel rat model of contrast-induced acute kidney injury, Ann. Transl. Med. 7 (2019).

[56] R. Morizane, S. Fujii, T. Monkawa, K. Hiratsuka, S. Yamaguchi, K. Homma, H. Itoh, miR-34c attenuates epithelial-mesenchymal transition and kidney fibrosis with ureteral obstruction, Sci, Rep 4 (2014) 1–9.

[57] E.-J. Park, H.J. Jung, H.-J. Choi, J.-I. Cho, H.-J. Park, T.-H. Kwon, miR-34c-5p and CaMKII are involved in aldosterone-induced fibrosis in kidney collecting duct cells, Am. J. Physiol. Physiol. 314 (2018) F329–F342.

[58] X.-D. Liu, L.-Y. Zhang, T.-C. Zhu, R.-F. Zhang, S.-L. Wang, Y. Bao, Overexpression of miR-34c inhibits high glucose-induced apoptosis in podocytes by targeting Notch signaling pathways, Int. J. Clin. Exp. Pathol. 8 (2015) 4525.

[59] X.-L. Hu, X.-X. Wang, Y.-M. Zhu, L.-N. Xuan, L.-W. Peng, Y.-Q. Liu, H. Yang, C. Yang, L. Jiao, P.-Z. Hang, MicroRNA-132 regulates total protein of Nav1. 1 and Nav1. 2 in the hippocampus and cortex of rat with chronic cerebral hypoperfusion, Behav. Brain Res. 366 (2019) 118–125.

[60] Y. Cai, W. Wang, H. Guo, H. Li, Y. Xiao, Y. Zhang, miR-9-5p, miR-124-3p, and miR-132-3p regulate BCL2L11 in tuberous sclerosis complex angiomyolipoma, Lab. Investig. 98 (2018) 856–870.

[61] T.V. Eskildsen, P.L. Jeppesen, M. Schneider, A.Y. Nossent, M.B. Sandberg, P.B. L. Hansen, C.H. Jensen, M.L. Hansen, N. Marcussen, L.M. Rasmussen, Angiotensin II regulates microRNA-132/-212 in hypertensive rats and humans, Int. J. Mol. Sci. 14 (2013) 11190–11207.

[62] A. Ucar, V. Vafaizadeh, H. Jarry, J. Fiedler, P.A.B. Klemmt, T. Thum, B. Groner, K. Chowdhury, miR-212 and miR-132 are required for epithelial stromal interactions necessary for mouse mammary gland development, Nat. Genet. 42 (2010) 1101.

[63] A. Ichihara, M.S. Yatabe, The (pro)renin receptor in health and disease, Nat. Rev. Nephrol. 15 (2019) 693–712. https://doi.org/10.1038/s41581-019-0160-5.

[64] A.J. Miller, A.C. Arnold, The renin–angiotensin system in cardiovascular autonomic control: recent developments and clinical implications, Clin. Auton. Res. 29 (2019) 231–243.

[65] M. Hennrikus, A.A. Gonzalez, M.C. Prieto, The prorenin receptor in the cardiovascular system and beyond, Am. J. Physiol. Circ. Physiol. 314 (2018) H139–H145.

[66] M. He, L. Zhang, Y. Shao, X. Wang, Y. Huang, T. Yao, L. Lu, Inhibition of renin/prorenin receptor attenuated mesangial cell proliferation and reduced associated fibrotic factor release, Eur. J. Pharmacol. 606 (2009) 155–161.

[67] F. Riediger, I. Quack, F. Qadri, B. Hartleben, J.-K. Park, S.A. Potthoff, D. Sohn, G. Sihn, A. Rousselle, V. Fokuhl, Prorenin receptor is essential for podocyte autophagy and survival, J. Am. Soc. Nephrol. 22 (2011) 2193–2202.

[68] Y. Oshima, K. Kinouchi, A. Ichihara, M. Sakoda, A. Kurauchi-Mito, K. Bokuda, T. Narita, H. Kurosawa, G.-H. Sun-Wada, Y. Wada, Prorenin receptor is essential for

normal podocyte structure and function, J. Am. Soc. Nephrol. 22 (2011) 2203–2212.
[69] X.-Q. Li, W. Tian, X.-X. Liu, K. Zhang, J.-C. Huo, W.-J. Liu, P. Li, X. Xiao, M.-G. Zhao, W. Cao, Corosolic acid inhibits the proliferation of glomerular mesangial cells and protects against diabetic renal damage, Sci. Rep. 6 (2016) 1–16.
[70] K. Kinouchi, A. Ichihara, M. Sano, G.-H. Sun-Wada, Y. Wada, A. Kurauchi-Mito, K. Bokuda, T. Narita, Y. Oshima, M. Sakoda, The (pro) renin receptor/ATP6AP2 is essential for vacuolar H+-ATPase assembly in murine cardiomyocytes, Circ. Res. 107 (2010) 30–34.
[71] J. Zhang, J. Wu, C. Gu, N.A. Noble, W.A. Border, Y. Huang, Receptor-mediated nonproteolytic activation of prorenin and induction of TGF-β1 and PAI-1 expression in renal mesangial cells, Am. J. Physiol. Physiol. 303 (2012) F11–F20.
[72] R.A. Melnyk, J. Tam, Y. Boie, B.P. Kennedy, M.D. Percival, Renin and prorenin activate pathways implicated in organ damage in human mesangial cells independent of angiotensin II production, Am. J. Nephrol. 30 (2009) 232–243.
[73] M.K. Ames, C.E. Atkins, B. Pitt, The renin-angiotensin-aldosterone system and its suppression, J. Vet. Intern. Med. 33 (2019) 363–382.
[74] V. Agarwal, G.W. Bell, J.-W. Nam, D.P. Bartel, Predicting effective microRNA target sites in mammalian mRNAs, Elife 4 (2015) e05005.
[75] J. Gerardo-Aviles, S. Allen, P.G. Kehoe, Renin-angiotensin system microRNAs, special focus on the brain, Renin-Angiotensin Syst. Present Futur. (2017) 173–199.
[76] Y. Wang, E.R. Lumbers, A.L. Arthurs, C. Corbisier de Meaultsart, A. Mathe, K. A. Avery-Kiejda, C.T. Roberts, F.B. Pipkin, F.Z. Marques, B.J. Morris, Regulation of the human placental (pro) renin receptor-prorenin-angiotensin system by microRNAs, MHR Basic Sci. Reprod. Med. 24 (2018) 453–464.
[77] Y. Li, X. Jiang, L. Song, M. Yang, J. Pan, Anti-apoptosis mechanism of triptolide based on network pharmacology in focal segmental glomerulosclerosis rats, Biosci. Rep. 40 (2020).
[78] S. Robertson, S.M. MacKenzie, S. Alvarez-Madrazo, L.A. Diver, J. Lin, P.M. Stewart, R. Fraser, J.M. Connell, E. Davies, MicroRNA-24 is a novel regulator of aldosterone and cortisol production in the human adrenal cortex, Hypertension 62 (2013) 572–578.
[79] G.G. Braliou, A.-M.G. Grigoriadou, P.I. Kontou, P.G. Bagos, The role of genetic polymorphisms of the Renin–Angiotensin System in renal diseases: a meta-analysis, Comput. Struct. Biotechnol. J. 10 (2014) 1–7.
[80] L.J. Smyth, M. Cañadas-Garre, R.C. Cappa, A.P. Maxwell, A.J. McKnight, Genetic associations between genes in the renin-angiotensin-aldosterone system and renal disease: a systematic review and meta-analysis, BMJ Open 9 (2019), e026777.
[81] M. Pacurari, P.B. Tchounwou, Role of microRNAs in renin-angiotensin-aldosterone system-mediated cardiovascular inflammation and remodeling, Int. J. Inflamm. 2015 (2015).
[82] P.L. Jeppesen, G.L. Christensen, M. Schneider, A.Y. Nossent, H.B. Jensen, D. C. Andersen, T. Eskildsen, S. Gammeltoft, J.L. Hansen, S.P. Sheikh, Angiotensin II type 1 receptor signalling regulates microRNA differentially in cardiac fibroblasts and myocytes, Br. J. Pharmacol. 164 (2011) 394–404.
[83] A.J. van Zonneveld, Y.W. Au, W. Stam, S. van Gelderen, J.I. Rotmans, P.M.T. Deen, T.J. Rabelink, R. Bijkerk, MicroRNA-132 regulates salt-dependent steady-state renin levels in mice, Commun. Biol. 3 (2020) 1–11.
[84] M. Abuzeineh, A. Aala, S. Alasfar, N. Alachkar, Angiotensin II receptor 1 antibodies associate with post-transplant focal segmental glomerulosclerosis and proteinuria, BMC Nephrol. 21 (2020) 1–8.
[85] Y. Liu, F. Wang, P. Liu, A.M. Geurts, J. Li, A.M. Williams, K.R. Regner, Y. Kong, H. Liu, J. Nie, MicroRNA-214-3p in the kidney contributes to the development of hypertension, J. Am. Soc. Nephrol. 29 (2018) 2518–2528.
[86] R. Nosalski, M. Siedlinski, L. Denby, E. McGinnigle, M. Nowak, A.N.D. Cat, L. Medina-Ruiz, M. Cantini, D. Skiba, G. Wilk, T-cell–derived miRNA-214 mediates perivascular fibrosis in hypertension, Circ. Res. 126 (2020) 988–1003.